Spectroscopic Characterization of GaAs/AlGaAs APDs with Separate Absorption and Multiplication Regions

C. Nichetti[a,b], T. Steinhartová[b,c], M. Antonelli[a], D. De Angelis[b], G. Cautero[a,d], G. Biasiol[c], A. Pilotto[f], F. Driussi[f], P. Palestri[f], L. Selmi[g], F. Arfelli[b,d] and R.H. Menk[a,d,e]

a) Elettra-Sincrotrone Trieste S.C.p.A, Area Science Park Basovizza, 34149 Trieste, Italy b) Department of Physics, University of Trieste, 34128 Trieste, Italy c) IOM CNR, Laboratorio TASC, Area Science Park Basovizza, 34149 Trieste, Italy d) Istituto Nazionale di Fisica Nucleare, INFN Sezione di Trieste, Trieste, 34100, Italy e) Department of Medical Imaging, University of Saskatchewan, Saskatoon, SK S7N 5A2, Canada f) DPIA, University of Udine, Udine, Italy g) DIEF, University of Modena and Reggio Emilia, Via Trovarelli 2, 44100 Modena, Italy

GaAs/AlGaAs Avalanche Photodiode

- **Avalanche photodiodes (APDs)** provide an internal multiplication **gain** due to **impact ionization**. If the associated multiplication noise is low, they present advantages over external amplification.
- APDs for detection in the X-ray regime, especially for applications in **synchrotron radiation**, are traditionally based on Si as it is the most mature technology and has low noise associated to the multiplication process.
- The characteristics of last-generation light sources pose more stringent requirements in terms of detectable **energies**, response **times** and radiation **hardness** and this has led to the research of new materials: **compound-semiconductors** (e.g. GaAs/AlGaAs hetero-junctions) were suggested [1, 2].

Problem: to obtain low-noise APDs it is essential to have very different electron and hole ionization coefficients [1]. Unfortunately, in III-V compound semiconductors their ratio is close to one.

Solution: band-engineered heterostructures consisting of alternating GaAs/AlGaAs nanometric layers have been proposed, in order to effectively enhance electron multiplication at interfaces and hinder hole multiplication [3].

Separate Absorption and Multiplication APD

Fig. 1. (a) Sketch of the fabricated avalanche photodiode with separate absorption and multiplication regions. (b) Scheme of the structure grown by MBE. (c) Band diagram under reverse bias.

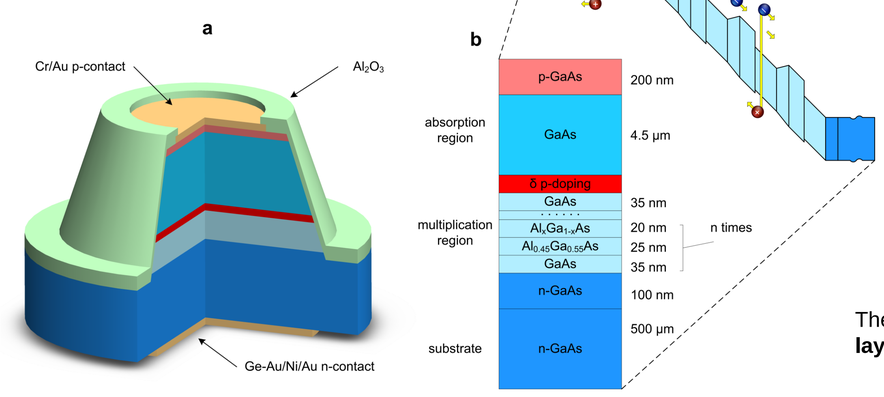

The SAM APD [4] is a structure with **Separate**

- **Absorption** region: a 4.5-μm-thick GaAs layer
- **Multiplication** region: a staircase structure with different repetitions. Each stage consists of
  - 35 nm GaAs
  - 25 nm $Al_{0.45}Ga_{0.55}As$
  - 20 nm linearly graded $Al_xGa_{1-x}As$ region (digital alloy).

device	A	B	C
steps	6	12	24
capacitance [pF]	~6	~4	~2
break down [V]	19	38	60

The two regions are electrically separated by a **p-doped layer** under the form of a δ sheet of C atoms.

X-ray measurements

To assess the response to high energy photons, the devices B were tested under **hard X-rays** generated by the XRD2 wiggler beamline at Elettra Sincrotrone Trieste [5] (12.4 keV and 1.71013ph·s^{-1} over an area of 300x90 m^2).

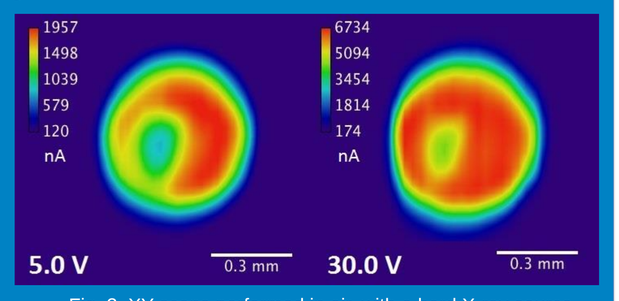

Fig. 2. XY scans performed in air, with a hard X-ray source (12.4 keV) at different bias voltages.

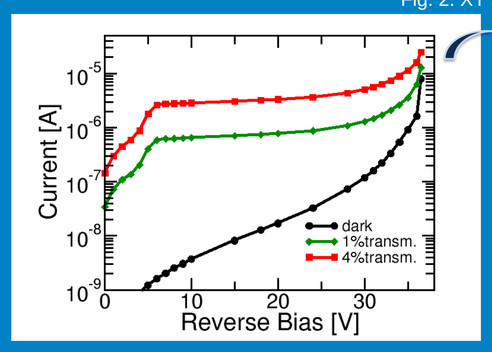

Fig. 3. Measurements performed in air with a hard X-ray beam provided by the XRD2 beamline: black circles, dark current; green diamonds, 1% of transmitted beam; red squares, 4 times higher than the previous one.

The IV curve under illumination follows qualitatively the expected progression of a SAM APD:

- recombination (V_{bias} < 4V),
- unity gain (4V < V_{bias} < 7V),
- punch through (V_{bias} 7V), where all charges generated in the absorption region are transferred into the multiplication region,
- avalanche region (7V < V_{bias} < 38V)
- breakdown (V_{bias} > 38V) after which the device can operate in Geiger mode.

Measurement Set-up

The measurement set-up consist of a

- Low-noise power supply
- Low-noise charge-sensitive preamplifier (CSA)
- CSA bias board
- Shaper
- Oscilloscope

For tests under illumination the devices were mounted on a dedicated PCB. As preliminary test a pulsed **green table top laser (200 kHz, 540 nm)** was used to emulate a X-ray single photon source (^{55}Fe).

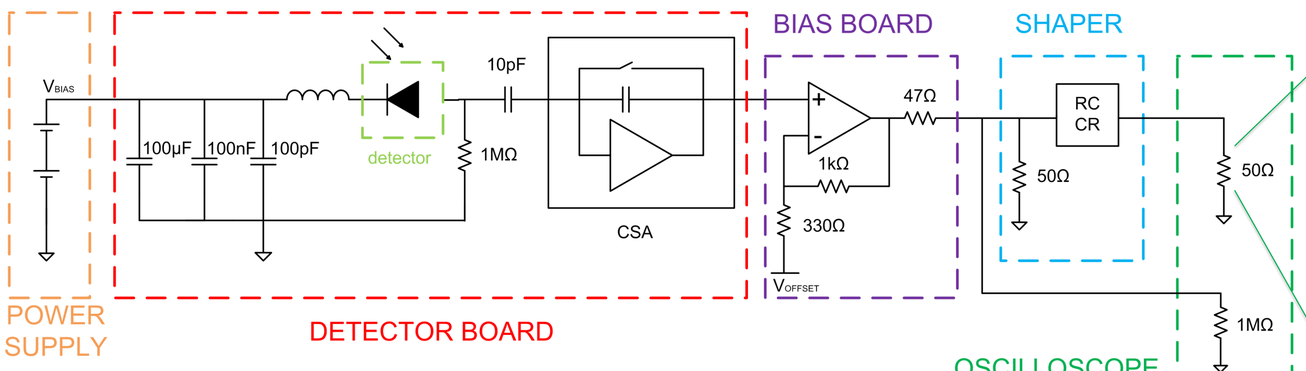

Fig. 4. Measurements set-up.

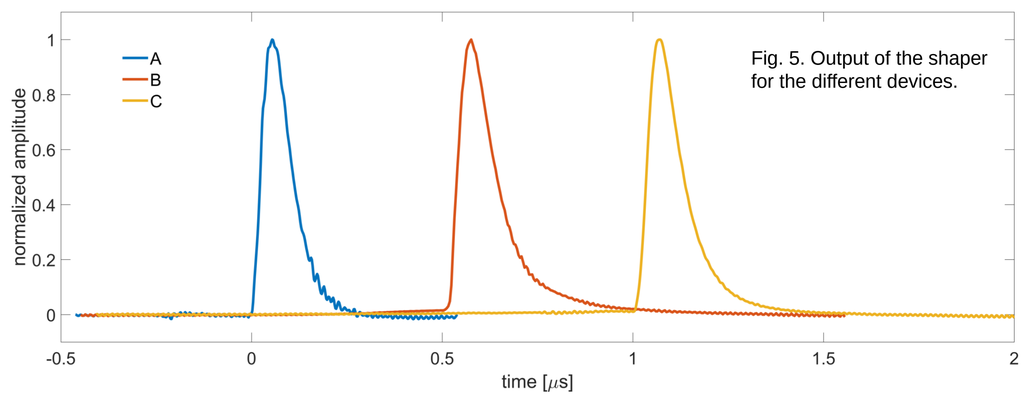

Fig. 5. Output of the shaper for the different devices.

Histograms

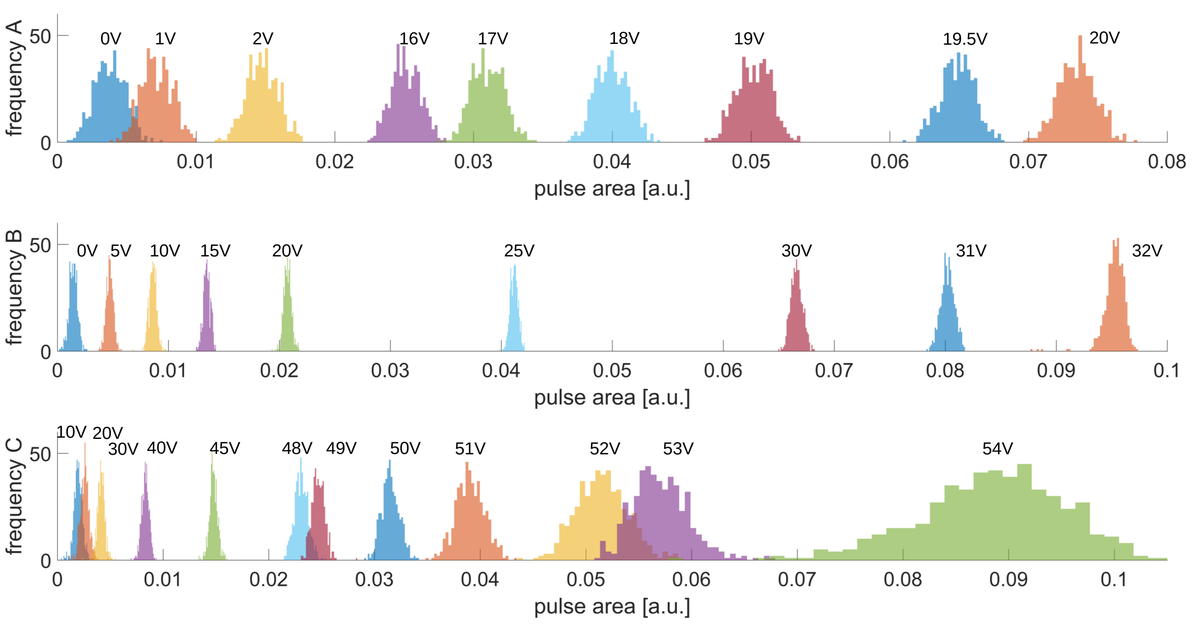

Fig. 6. Histogram of the area of the pulses resulting from the shaper, for devices A, B, C, respectively.

- **Device A**: it is limited by the noise of the set up (the deviation is almost constant for all biases)
- **Device B**: the multiplication noise becomes more evident (a minimum increase in the deviation can be noticed)
- **Device C**: the histograms depend strongly on the gain of the device (the deviations at higher biases are evidently larger)

Gain and SNR

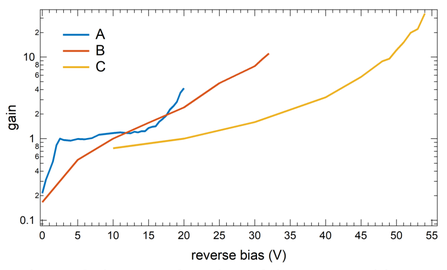

Fig. 7. Gains as a function of the reverse bias.

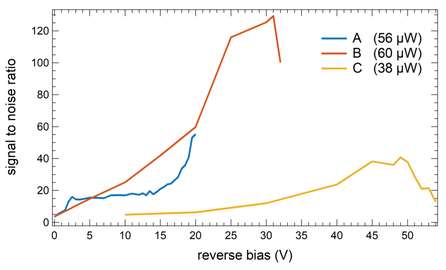

Fig. 8. SNR as a function of the reverse bias.

The gain increases with the number of steps as it is reasonable. In fact the curve of the 6 step device (blue) reaches lower gain compared to the 24 steps one (yellow) before reaching the break down voltage.

Figure 8 shows how the signal to noise ratio (SNR) in the devices with a larger number of steps starts to decrease before the break down voltage, meanwhile for the 6 steps device this does not occur.

Conclusions

- A set-up for spectroscopic performance evaluation based on a CSA was built
- Preliminary test with a pulsed laser were performed at
  - 200 kHz repetition rate
  - 540 nm wavelength
- Increasing the number of steps allows to have higher gains and, in principle, to reduce the excess noise factor
- Further spectroscopic measurements will be carried out with high energy pulses
  - ^{55}Fe (characteristic fluorescence lines)
  - Alpha particles

Acknowledgments

The authors would like to thank the personal of the laser laboratory for the opportunity to perform some measurements and Giacomo Jarc for its support during the experiments. Italian MIUR, PRIN 2015 project 2015WMZ5C8.

REFERENCES

[1] R. McIntyre, IEEE Trans. Electron. Devices, 13, 164 (1966).
[2] P. Yuan, K. Anselm, C. Hu, H. Nie, C. Lenox, A. Holmes, B. Streetman, J. Campbell, and R. McIntyre, IEEE Trans. Electron. Devices, 46, 1632 (1999).
[3] F. Capasso, W.T. Tsang, G.F. Williams, IEEE Trans. Electron Devices 30 ,381, (1983).
[4] T. Steinhartova, C. Nichetti, M. Antonelli, G. Cautero, R. Menk, A. Pilotto, F. Driussi, P. Palestri, L. Selmi,K. Koshmak, S. Nannarone, F. Arfelli, S. Dal Zilio, and G. Biasiol, J. Instrum., 12, C11017 (2017).
[5] XRD2, “Elettra and FERMI lightsources,” (2018) .

CONTACT
camilla.nichetti@elettra.eu